Raman scattering from intercalated donor compounds of graphite*

R. J. Nemanich† and S. A. Solin‡
The Department of Physics and The James Franck Institute, The University of Chicago, Chicago, Illinois 60637

D. Güerard§
Moore School of Electrical Engineering and Laboratory for Research on the Structure of Matter, University of Pennsylvania, Philadelphia, Pennsylvania 19174

(Received 23 August 1976; revised manuscript received 26 October 1976)

Raman spectra of vibrational excitations in graphite intercalated with alkali donor atoms have been obtained at room temperature in the backscattering configuration using argon ion laser excitation. Stage 1, 2, and 3 cesium donor compounds prepared from highly oriented pyrolytic graphite (HOPG) were studied as were stage 1 and 2 HOPG potassium donor compounds. Second stage cesium and potassium intercalates exhibit a single Raman band unshifted from the E_{2g} intralayer mode of HOPG which occurs at 1582 cm^{-1}. In contrast, the third-stage cesium intercalate produces a doublet spectrum with one component upshifted from and the other at the same position as the HOPG intralayer mode. The above described observations for stage-2 and higher-stage donor compounds are explained by an analysis which considers (a) the nearest-layer configurations which a given carbon layer can experience in a given stage of intercalation, (b) the change in C-C bond distance with intercalation, and (c) the effect of intercalation on the carbon interlayer interaction. The spectra of stage-1 cesium and potassium intercalates are almost identical and each contains two anomolously shaped bands, one near to but down shifted from the interlayer mode of HOPG and one at ~ 560 cm^{-1}, both being superposed on a continuum background. These bands are attributed to Breit-Wigner or Fano resonances between an electronic Raman scattering continuum and the E_{2g} intralayer mode and an out of plane intralayer vibration, respectively. The parameters Γ, q, and $\bar{\Omega}$ governing the Breit-Wigner resonance are determined by fitting the observed line shapes of each of the two bands in the cesium and potassium intercalate spectra.

I. INTRODUCTION

Graphite, the prototype layered solid, can form lamellar compounds with many chemical substances of both atomic and molecular form which may be inserted between the hexagonal carbon planes.[1,2] Intercalated compounds of graphite are classified by the electrical character and structural arrangements of the intercalated substance. That substance is characterized as a donor or acceptor according to whether it contributes electron charge to or extracts charge from the graphite layer. There is a wealth of evidence that intercalated atoms or molecules enter the graphite structure as whole layers separated by one or more hexagonal graphite layers.[1,2] Therefore graphite intercalate compounds are also designated by the number of carbon layers per layer of intercalate or the "stage" of intercalation. For instance a first stage compound would consist of alternating layers of carbon atoms and intercalate while two layers of carbon atoms would separate layers of intercalate in a second-stage compound. Intercalates of graphite are additionally structurally classified as lamellar or residue compounds. Even the best crystals of graphite contain significant concentrations of structural defects.[3] Ubbelohde has noted[1] that additive species can be bound to such defects. When lamellar compounds formed in equilibrium with the vapor or liquid of the intercalated species are exposed to air or vacuum most but not all of the inserted atoms or molecules deintercalate. The resultant material is called a residue compound.

Intercalated compounds of graphite are of practical interest because the electrical properties of pristine graphite are drastically altered with intercalation. For instance, the low-temperature basal-plane a-axis conductivity can be increased with intercalation of potassium by approximately a factor of 20 to achieve values in the range exhibited by metals such as nickel.[4] Intercalated compounds of graphite are of fundamental interest for several reasons: (a) Some intercalates form well-characterized three-dimensional superlattices of stacked two-dimensional layers; (b) intercalated specimens constitute a controlled perturbation with which to study the properties of pristine graphite; and (c) graphite intercalates are excellent compounds with which models for the physics of two-dimensional ordered and disordered systems can be tested. For these and other reasons, intercalated graphite has been the focus of a considerable amount of research activity during the past two decades most notably that of Ubbelohde and co-workers[1] and Hennig and co-workers.[2] However, the bulk of the research efforts to date address the electrical, optical, structural, magnetic, and thermal properties of the crystal com-

TABLE I. Characterization of the graphite intercalate samples studied.

Samples	Graphite form	Stage	Intralayer modes (±1 cm^{-1})	Stage determined from	Comments
C_8K	HOPG	1	1547 [a]	x ray	
$C_{24}K$	HOPG	2	1599	x ray	
C_8Cs	HOPG	1	1519 [a]	x ray	
$C_{24}Cs$	HOPG	2	1598	Color	Obtained from C_8Cs with local heating in laser beam
$C_{36}Cs$	HOPG	3	1579, 1604	x ray	

[a] Position of (see Table III and text).

pounds.[5-7] Surprisingly, though the vibrational excitations of pristine graphite should be quite sensitive to intercalation they have till now aroused little research interest.[8,9] Accordingly in this paper we report on light-scattering studies of the vibrational excitations of lamellar compounds of graphite intercalated with the donor species potassium or cesium.

II. EXPERIMENTAL DETAILS

Samples of C_8K, $C_{36}Cs$, C_8Cs, and $C_{24}K$ were prepared in sealed Pyrex tubes by exposing thin rectangular plates of highly oriented stress-annealed pyrolytic graphite to the vapors of vacuum distilled potassium or cesium. The stage of intercalation of the compounds studied was determined from the c-axis dilation observed using x-ray diffraction and was confirmed by the uniform and characteristic colors of the low-stage alkali compounds. The samples studied in this work are characterized in Table I.

The Raman measurements reported here were performed in the brewster angle backscattering configuration using a cylindrically focussed 5145-Å argon ion laser incident beam, Jarrel-Ash model 25-100 double monochromator equipped with Jobin Yvon holographic gratings and photon counting detection electronics. The apparatus has been described in detail elsewhere.[10]

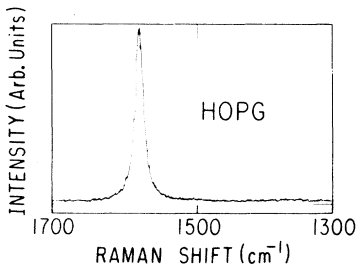

FIG. 1. Room-temperature Raman spectra of highly oriented pyrolytic graphite. Except where noted otherwise this spectrum and those which follow have abscissas which are linear in wavelength rather than wave number and were excited with the 5145-Å argon ion laser line.

III. RESULTS AND DISCUSSION

A. Raman spectra

The Raman spectrum of stress-annealed pyrolytic graphite is shown in Fig. 1. It contains only one sharp feature at 1582 cm^{-1}.[11,12] The Raman spectra of highly oriented pyrolytic graphite (HOPG) intercalated with K and Cs are shown, respectively, in Figs. 2(a)–2(d) for frequency shifts in the range 1200–1800 cm^{-1}. Their features are quite distinct from those of pure graphite. The spectrum of $C_{36}Cs$ not only exhibits a weak line at ~1580 cm^{-1}, the approximate position of the intralayer mode of pristine graphite but also shows a strong peak shifted to *higher* energy at 1604 cm^{-1}. In contrast the spectrum of $C_{24}K$ exhibits a lone relatively sharp band which also is upshifted in energy from the lone band of

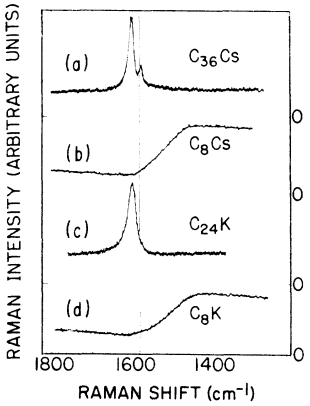

FIG. 2. Intralayer mode region room-temperature Raman spectra of graphite intercalates. The vertical line denotes the position of the intralayer mode of pristine graphite.

pristine HOPG. Finally the spectra of C_8Cs and C_8K shown in Figs. 2(b) and 2(d), respectively, exhibit clearly unique qualities with respect to the spectra of Figs. 2(a) and 2(c). No sharp peak is evident in the 1580-cm^{-1} region however a broad anomalous band shape is observed with a peak intensity at ~ 1430 cm^{-1}.

B. Effect of exposure to high laser power

The spectra of cesium and potassium intercalates exhibit interesting transformations as the laser power density is increased and the sample is heated locally. As can be seen from Fig. 3, when the laser power is increased from 120 to 520 mW the highly asymmetric band of first stage Cs intercalate transforms to a single slightly asymmetric band upshifted in energy from the band in pristine graphite and identical to the spectrum of $C_{24}K$ [Fig. 2(c)]. This transformation also occurs for the K intercalate but is incomplete at a power level of 70 mW (see Fig. 3). After exposure to high laser power the illuminated sample region no longer had the characteristic metallic gold luster of a first-stage alkali atom intercalate but rather had the metallic blue-black appearance of second-stage material. Apparently the local heating produced by the higher laser power promoted deintercalation and the transformation from first to second stage. The ejected alkali atoms ultimately deposited as a noticeable film on the inner surface of the sample ampule. It should be clear from the above discussion that extreme care and relatively low laser power levels must be employed to acquire the spectra of C_8K and C_8Cs.

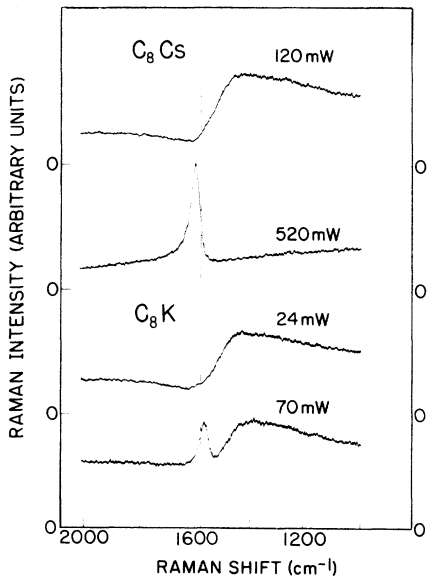

FIG. 3 Effect of laser power density on HOPG C_8Cs and C_8K. The vertical bar denotes the position of the intralayer mode of pristine HOPG.

C. Pristine graphite

To interpret the observations of Figs. 1–3 we must first describe the structural and vibrational properties of pristine graphite. The structure of ideal single-crystal graphite which has a four-atom hexagonal primitive cell of D_{6h}^4 space group[13] symmetry is shown in Fig. 4(a). The zone-center optic lattice vibrations of this structure have been analyzed by Brillson *et al.*[12] The vibrational modes can be decomposed into the following irreducible representations:

$$\Gamma = 2A_{2u} + 2B_{2g} + 2E_{1u} + 2E_{2g}, \quad (1)$$

of which there are three acoustic modes $A_{2u}+E_{1u}$, four Raman-active modes $2E_{2g}$, three infrared-active modes $A_{2u}+E_{1u}$, and two silent modes $2B_{2g}$. The atomic displacements associated with each normal mode have also been deduced by Brillson *et al.*,[12] and their results are displayed for future reference in Fig. 4. There are two first-order doublet Raman-active optic modes of E_{2g} symmetry. One of these E_{2g_2} in Fig. 4(b) corresponds to an in-plane intralayer mode and occurs at 1574 cm^{-1} in single-crystal graphite[11,12] and at 1582 cm^{-1} in HOPG (see Fig. 1). The other labeled E_{2g_1} in Fig. 4(b) is a rigid-layer vibration

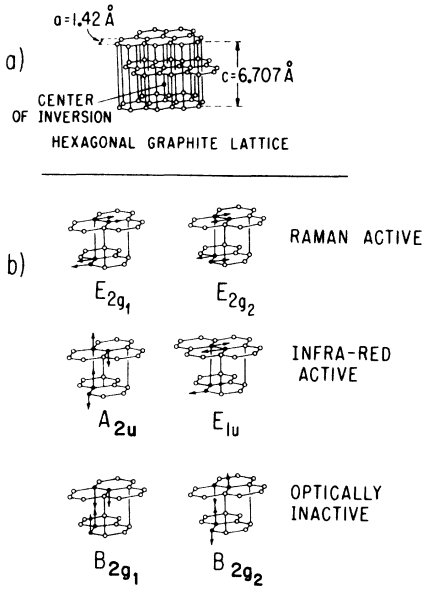

FIG. 4. (a) The crystal structure of graphite; (b) symmetry species and atomic displacements of the optical eigenmodes of graphite. All diagrams in this figure except the one for the B_{2g_1} mode are reproduced from Ref. 13.

and though Raman active has not been detected to date with light-scattering techniques. Neutron scattering measurements however have located that mode at ~ 45 cm^{-1}.[14]

D. Intercalated graphite

When pristine graphite is intercalated the nearest layer environment of carbon layers in the intercalated compound will depend on the stage of intercalation but is restricted to one of the three configurations specified in Table II. While stage-1 and -2 compounds each contain a single type of nearest layer configuration, labeled types *A* and *B*, respectively, in Table II, stage-3 and higher-stage compounds will contain two types of configuration one type *B* identical to that found in stage-2 material and one type *C* identical to that found in pristine graphite. In addition, though adjacent carbon layers in pristine graphite adopt the so-called staggered configuration in which the carbon hexagons in one layer, when viewed along the *C* axis, are displaced laterally with respect to the hexagons in immediately adjacent layers, carbon layers on either side of an alkali atom intercalated layer adopt the eclipsed configuration.[15] However, there is no case to our knowledge in which contiguous carbon layers adopt the eclipsed configuration.

Of the intercalate spectra which exhibit quasi-symmetric bands those of stage-2 HOPG Cs and K intercalates as noted earlier consist of a single upshifted band. Note from Fig. 2(c), Fig. 3, and Table I that the displacement of that band from the intralayer mode of pristine HOPG is 17 ± 3 cm^{-1}. That shift is within the bounds of the energy difference between the E_{1u} infrared active mode at 1588 ± 5 cm^{-1} and the E_{2g_2} Raman mode at 1574 ± 1 cm^{-1}.[12] The former mode involves a motion in which the atomic displacements of nearest neighbors in adjacent layers are in phase whereas they are out of phase for the latter (see Fig. 4). Thus to first order the interlayer interaction does not perturb the E_{1u} mode but depresses the frequency of the E_{2g} mode. The E_{2g_2} and E_{1u} modes would be degenerate in two-dimensional noninteracting layers. It is plausible then that the increase in intralayer frequency of pristine graphite upon alkali atom intercalation results from a reduction of the intralayer interaction associated with the increased spacing between carbon layers. In stage-2 material there is only one type of carbon layer, type *B*, which is located between another carbon layer and an intercalate layer. Thus only one upshifted Raman line is observed in stage-2 material. In contrast stage-3 $C_{36}Cs$ contains carbon layers in two distinct nearest layer environments. Therefore the spectrum of stage-3 $C_{36}Cs$ [Fig. 2(a)] shows two lines one at 1579 ± 2 cm^{-1}, which is the approximate position 1579 ± 2 cm^{-1} of the intralayer mode of pristine HOPG and may arise from excitations of type-*C* layers and one upshifted to 1603 ± 2 cm^{-1} which is ascribed to type-*B* layers.

In the foregoing we have considered only nearest layer contributions to the interlayer interaction. The neglect of more distant layers is justified for two reasons. First, the interlayer interaction, being of the van der Waals type decreases rapidly with interlayer distance; second, with respect to the central carbon layer in a type-*B* configuration, the second nearest layers are in an eclipsed configuration[15] as shown in Fig. 5 and will not contribute to the $E_{1u} - E_{2g_2}$ splitting because atoms in those layers move in phase with their nearest neighbors in the layer in question.

The single band and upshifted intralayer frequency of $C_{24}K$ and $C_{24}Cs$ are consistent with the recent x-ray measurements of Nixon and Parry who found that the intralayer C-C bond distance in C_nK increased with decreasing n or stage num-

TABLE II. Nearest layer configurations for carbon layers in lamellar compounds of graphite.

	——— Carbon layer ------ Intercalate layer		
Label	*A*	*B*	*C*
Nearest Layer	---- ——	—— ——	—— ——
Configuration	---- ——	---- ——	—— ——
Stage	$n = 1$	$n \geq 2$	$n \geq 3$

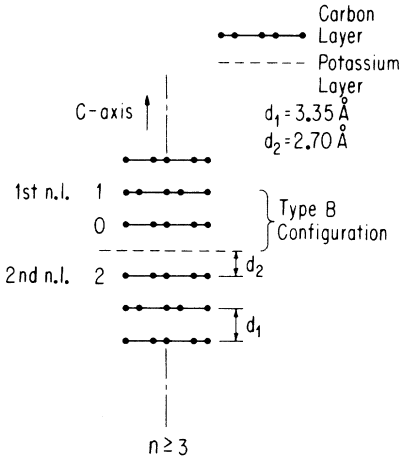

FIG. 5. Carbon layer and alkali layer stacking arrangements and nearest layer (nl) environments in stage n, $n \geq 3$, alkali-atom graphite crystal compounds (see also Table II).

ber.[16] They also noted that donated electrons were delocalized throughout the carbon layers which separated potassium layers. Thus each stage exhibited a single C-C distance which was the same for any carbon layer whether or not it was contiguous to or removed from a potassium layer. The increase in C-C bond distance can actually contribute to the upshift in the intralayer mode frequency as we now show.

The coefficients of linear expansion perpendicular to the hexagonal axis $\alpha_\perp$ of both single-crystal graphite[17] and HOPG[18] are negative at low temperatures. Therefore on cooling pristine graphite from room-temperature to liquid-helium temperature, the C-C bond distance increases. Usually an increase in bond length results in a weakening of the bond and a decrease in mode frequency.[19,20] In Fig. 6 we show the Raman spectrum of the intralayer mode of HOPG recorded at room temperature and 12 °K. Notice that in contrast to the anticipated behavior the intralayer mode shifts to higher frequency by 2.6 ± 1.5 cm^{-1} with a decrease in temperature and an increase in C-C bond length. This result while unusual indicates that the negative off-diagonal terms in the anharmonic Hamiltonian[20] have a nonnegligible effect on the intralayer vibration. Such an effect is consistent with the complicated atomic motions of the intralayer mode. If the frequency upshift exhibited by intercalates was dependent on the C-C bond distance then the position of the upshifted mode would vary with the stage of alkali-atom intercalation. While there is some indication that the shifts of the intralayer modes of type-*B* layers in $C_{24}Cs$ and $C_{36}Cs$ differ, that difference is not experimentally significant enough to establish definitively that the frequency upshift is dependent on the stage of intercalation.

We now address the anomalously shaped spectra of the stage-1 alkali-atom crystal compounds of graphite. Though we have so far concentrated on the intralayer mode at ~1600 cm^{-1} the analysis of those spectra is facilitated by a consideration of the entire Raman profile extending to zero frequency shift. Therefore we present in Fig. 7 the full spectra of HOPG C_8Cs and C_8K. The two spectra are remarkably similar and exhibit an additional anomalously shaped line at ≈ 560 cm^{-1} superposed upon a continuum background. Since the intercalated species in C_8K and C_8Cs is atomic, the full spectra of those materials should contain no bands associated with internal modes of vibration. Moreover, the first stage intercalates contain layers of six fold coordinated alkali atoms arranged in a hexagonal two-dimensional lattice[15] the primitive cell of which contains only one alkali atom. Such a structure will produce no optic vibrational modes and equivalently no first-order Raman spectrum. Thus the modes at ≈ 560 cm^{-1} in the spectra of Fig. 7 cannot be associated with alkali layer excitations. In addition those modes appear at almost the same Raman shift in C_8K and C_8Cs while Cs and K have much different atomic masses. The ≈ 560-cm^{-1} mode must therefore result from an excitation of the graphite layers. The first-order Raman spectrum of pristine HOPG graphite contains no lines below 1580 cm^{-1} as can be seen from Fig. 8 (which also shows for future reference the full Raman spectra of $C_{24}Cs$, $C_{24}K$, and $C_{36}Cs$). Recent calculations indicate that the dominant peak in the one phonon density of out of plane vibrational states of graphite occurs at approximately 500 cm^{-1}.[21,22] However, the uncertainty in that value is large and is a manifestation of the uncertainty in the force constants used to calculate the phonon dispersion curves of graphite.[21,22] No neutron scattering data is available for frequencies above 450 cm^{-1}. Nevertheless, it is an out of plane vibration that would be most

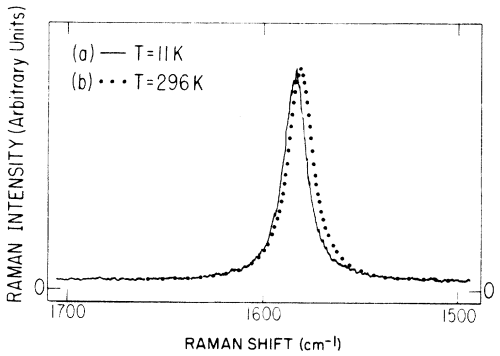

FIG. 6. Temperature dependence of the Raman spectrum of highly oriented pyrolytic graphite. The abscissa is linear in wave number. Spectra (a) and (b) were excited with 5145- and 4880-Å radiation, respectively.

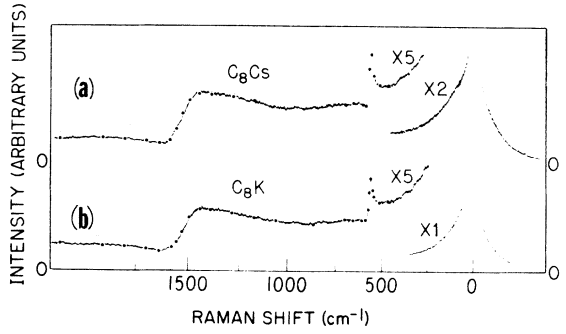

FIG. 7. Full Raman spectra of (a) HOPG C_8Cs; and (b) HOPG C_8K. The dots are obtained from a theoretical fit using Eqs. (2) with Γ and q as adjustable parameters and the background indicated by the dashed line. See also Table III.

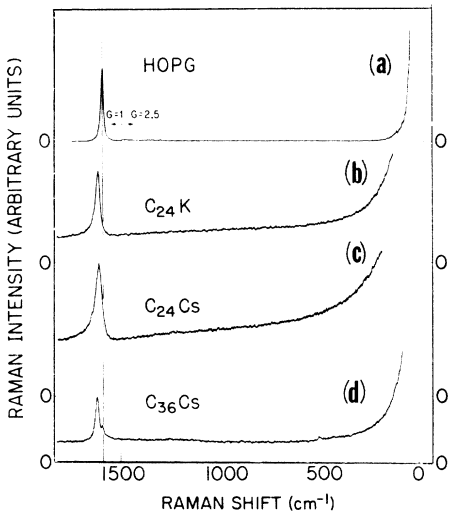

FIG. 8. Full Raman spectra of (a) HOPG; (b) HOPG $C_{24}K$; (c) HOPG $C_{24}Cs$ obtained from C_8Cs with high-power density illumination; and (d) HOPG $C_{36}Cs$.

perturbed and possibly Raman activated by the presence of alkali-atom layers in the intercalated first-stage material. There is no hint whatsoever of the 566-cm^{-1} line in the spectra of lower than stage-1 HOPG compounds as can be seen from Fig. 8. We will return again to this point after addressing the band shapes shown in Fig. 7.

The anomalous asymmetric shape of the band at ~560 cm^{-1} as well as that of the intralayer mode in Fig. 7 is characteristic of a Breit-Wigner[23] or Fano[24] interference that develops when a discrete level interacts with a continuum of states. The theory for the line shape that results when such an interaction occurs has been reviewed several times, most recently by Cerdiera *et al.*[25] and Scott[26] and is briefly summarized as follows: Suppose that transitions between a ground initial state $|0\rangle$ and a continuum of states $|f\rangle$ can occur through two channels one involving an intermediate discrete state $|m\rangle$ which lies within the energy range of the continuum and one direct. If these transitions are associated with a Raman process the Raman cross section $\sigma(q,\epsilon)$ is given by

$$\sigma(q,\epsilon)=\sigma_2(q+\epsilon)^2/(1+\epsilon^2)+\sigma_2^1, \tag{2a}$$

where

$$q=\langle m|\alpha_{ij}^1|0\rangle/\pi^2 W\langle f|\alpha_{ij}^2|0\rangle \tag{2b}$$

and

$$\epsilon=(1/\pi)(\omega-\bar{\Omega})/|W|^2=(\omega-\bar{\Omega})/\Gamma, \tag{2c}$$

while $\Gamma=\pi|W|^2$ is a linewidth parameter, σ_2 is the scattering cross section for the resonance, and σ_2' is the scattering cross section for the continuum spectrum. Also W is the transition rate between the discrete and continuum states, $\bar{\Omega}$ is the renormalized resonance frequency, and α_{ij}^1 and α_{ij}^2 are the differential polarizability tensor operators for discrete and continuum scattering processes.

There are many examples of Breit-Wigner resonances in solid-state physics particularly those in which a discrete one-phonon state interacts with either a two-phonon continuum[27,28] or a continuum of electronic states.[29,30] We believe the spectra of Fig. 7 are examples of the latter. The continuum spectrum on which the Breit-Wigner resonances are superposed is clearly evident in Fig. 7, and is attributed to electronic Raman scattering[30] from the metallic sample. Continuum electronic Raman scattering has been observed from interband electronic transitions[25] and single-particle intraband excitations.[31,32] The continuum spectrum that arises from interband transitions has a low-energy cutoff determined by the band separation at the Fermi level. In contrast, the single-particle intraband scattering extends down to zero frequency shift. The low-frequency Stokes-Anti-Stokes spectra of C_8Cs and C_8K are shown in Fig. 7 on a reduced amplitude scale. Notice that each spectrum is highly asymmetric with respect to the zero shift position and is thus due to true continuum scattering and not to parasitic scattering of the incident laser light. As can be seen from Fig. 7 the continuum scattering extends to the lowest measurable frequency and is probably due to single-particle scattering. However the continuum spectrum could conceivably arise from interband scattering with a very low minimum cutoff frequency. Since the band structure of the intercalate is not known it is impossible to definitively assign the continuum process.

To verify that the observed line shapes in Fig. 7 are indeed attributable to Breit-Wigner resonances we have fit the asymmetric lines in the C_8Cs and C_8K spectra using Eqs. (2) with Γ and q as adjustable parameters. The results of those fits together with the resulting value of $\bar{\Omega}$ are summarized in Table III. The fits, indicated by the solid circles in Fig. 7, were obtained by superposing the resonance shapes on the continuum background represented by the dashed line. This background was arbitrarily chosen to match the shape of the

TABLE III. Parameters of the Breit-Wigner or Fano resonances in the spectra of C_8K and C_8Cs.

Compound	C_8K		C_8Cs	
$\bar{\Omega}$ (cm^{-1})	566	1547	558	1519
Γ (cm^{-1})	9.1	78.7	9.7	95.6
q	−2.1	−0.8	−2.5	−1.0

spectrum and could in principle be calculated if the band structure of the intercalate was known. Given the uncertainty in the background the fit of theory to experiment in Fig. 7 is excellent.

The contrast between the spectra of first-stage alkali intercalates [Figs. 7(a) and 7(b)] and second-stage intercalates [Figs. 8(b) and 8(c)] is dramatic. The second-stage compounds clearly do exhibit a continuum background and there is some evidence of a Fano interaction between the continuum and the intralayer mode which is slightly asymmetric. The 560-cm^{-1} mode is completely absent from the spectra of Figs. 8(b) and 8 (c) as well as from the spectrum of third-stage $C_{36}Cs$ [Fig. 8(d)]. The three fold increase in donor concentration between stages 2 and 1 can account at least qualitatively for the larger continuum background in the latter. But the most significant distinction between stage-1 and stage-2 alkali-metal compounds is that intercalated layers of stage-2 and higher-stage material are disordered or liquidlike at room temperature whereas intercalated layers of stage-1 compounds are ordered at room temperature.[33-35] It is not clear at this time whether the stage-1 ordering or the increased charge density or a combination of both activates the 560-cm^{-1} mode. We can however conclude from the similarity in the spectra of C_8K and C_8Cs that the Raman process is insensitive to the three-dimensional c-axis stacking of intercalate layers. The stacking sequences of intercalate layers are different in C_8Cs and C_8K.[36]

E. Electron band-structure effects

For at least two decades the interpretation of the electrical, magnetic, thermoelastic, and other physical properties of graphite intercalates has been predicated upon analyses based on the electron band structure of the isolated layer[37] which has a π bonding conduction band that is degenerate with a π antibonding valence band at the corners of the hexagonal brillouin zone.[38] If there were indeed a relationship between the band structure of pristine graphite and that of intercalated graphite, the two-dimensional band-structure approach would only be justified because the interlayer interaction decreases upon intercalation. In terms of the two-dimensional band structure the increase in conductivity engendered by intercalation occurs as follows: donor intercalates populate the otherwise empty levels of the conduction band with electrons which of course enhance the conductivity; similarly, acceptor intercalates extract electrons from the filled (at 0 °K) valence band thereby creating free holes which also enhance the conductivity.

It is a straightforward matter to predict the effect of intercalation on the intralayer vibrational mode frequency of graphite if the two-dimensional band structure of a pristine graphite layer is preserved. For such a structure intercalation with a donor would populate antibonding states. Thus donors should weaken the intralayer forces and cause a reduction of the intralayer vibrational mode frequency in disagreement with our observations. In fact it appears that neither a two-dimensional band-structure model or for that matter a three-dimensional model such as that of Sloncewski and Weiss[39] is appropriate for low-stage graphite intercalates. Bach and co-workers have shown from ESCA (electron spectroscopy for chemical analysis) measurements that the electronic band structures of graphite is drastically altered upon intercalation with even small amounts of donor[40] impurities.

IV. CONCLUDING REMARKS

During the course of the above described measurements we have routinely scanned the region of the second-order Raman spectrum of graphite to ascertain what changes if any were caused by intercalation. Although there are features in the second-order Raman spectra of pristine HOPG which are about 40% as intense as the first-order intralayer mode band[22,41] all of the donor compounds showed a highly suppressed second-order Raman spectrum. The absence of a second-order spectrum for the donor crystal compounds studied cannot be ascribed to a reduction in the interlayer interaction attendant to intercalation. The dominant features in the second-order Raman spectrum of HOPG do not result from combinations or overtones involving rigid-layer excitations.[22] The effect of intercalation on the second-order Raman spectrum of graphite will be the subject of further study.

While we have shown that the Raman spectra of stage-2 and higher-stage compounds of graphite can be adequately interpreted without invoking an analysis based on the electronic band structure, the band structure of stage-1 donor compounds largely determines the shape of the continuum background and thus the spectral properties. There is thus a need for accurate calculations of the stage-1 alkali atom intercalate band structure. Such calculations should be feasible and would be facilitated by the propensity of alkali atoms to affix themselves to preferred sites in the crystal compound.

ACKNOWLEDGMENTS

Thanks are due to J. E. Fischer and M. H. Cohen for useful discussions. Thanks are also due A. W. Moore for providing us with pristine HOPG.

*Research supported by ERDA. It has also benefited from general support of the Materials Research Laboratory of the University of Chicago by the NSF.

†Present address: Xerox Palo Alto Research Center, Palo Alto, Calif.

‡Supported by the Alfred P. Sloan Foundation.

§Nato Visiting Scholar from the University of Nancy, France. Supported by NSF through the University of Pennsylvania Materials Research Lab: DMR 76-00678.

[1]A. R. Ubbelohde and F. A. Lewis, *Graphite and its Crystal Compounds* (Clarendon, Oxford, 1960).

[2]G. R. Hennig, in *Progress in Inorganic Chemistry*, edited by F. A. Cotton (Interstate, New York, 1959), Vol. I, p. 125.

[3]See Chap. I of Ref. 1 for a discussion of various defects that occur in graphite.

[4]G. K. White and S. B. Woods, Philos. Trans. R. Soc. Lond. A 251, 273 (1959).

[5]W. Rudorff, Adv. Inorg. Chem. Radiochem. 1, 223 (1959), and references therein.

[6]A. S. Bender and D. A. Young, J. Phys. C 5, 2163 (1972).

[7]J. J. Murray and A. R. Ubbelohde, Proc. R. Soc. A 312, 380 (1969).

[8]A preliminary report on this work was presented by S. A. Solin and R. J. Nemanich, Bull. Am. Phys. Soc. 20, 429 (1975).

[9]J. J. Song, D. D. L. Chung, and M. S. Dresselhaus, Bull. Am. Phys. Soc. 21, 339 (1976).

[10]D. M. Hwang and S. A. Solin, Phys. Rev. B 7, 843 (1972).

[11]F. Tunistra and J. L. Koenig, J. Chem. Phys. 53, 1126 (1970).

[12]L. L. Brillson, E. Burstein, A. A. Maradudin, and T. Stark, in *Physics of Semimetals and Semiconductors*, edited by D. L. Carter and R. T. Bate (Pergamon, Oxford, 1971), p. 187.

[13]R. W. G. Wyckoff, *Crystal Structures* (Oxford U. P., Oxford, 1962), Vol. I, p. 26.

[14]G. Dolling and B. N. Brockhouse, Phys. Rev. 128, 1120 (1962); also N. Wakabayashi, H. G. Smith, and R. M. Nicklow, Bull. Am. Phys. Soc. 17, 292 (1972).

[15]W. Rüdorff and E. Schulze, Z. Anorg. Chem. 277, 156 (1954).

[16]D. E. Nixon and G. S. Parry, J. Phys. C 2, 1732 (1969).

[17]J. B. Nelson and D. P. Riley, Proc. Phys. Soc. Lond. 57, 477 (1945).

[18]B. T. Kelly, W. H. Martin, and P. T. Nettley, Philos. Trans. R. Soc. Lond. A 260, 37 (1966).

[19]R. Zallen, Phys. Rev. B 9, 4485 (1974).

[20]G. Leibfried and W. Ludwig, Solid State Phys. 12, 276 (1961).

[21]R. Nicklow, N. Wakabayashi, and H. G. Smith, Phys. Rev. B 5, 4951 (1972).

[22]R. J. Nemanich and S. A. Solin (unpublished).

[23]G. Breit and E. Wigner, Phys. Rev. 49, 519 (1936).

[24]U. Fano, Phys. Rev. 124, 1866 (1961).

[25]F. Cerdeira, T. A. Fjeldly, and M. Cardona, Phys. Rev. B 8, 4734 (1973).

[26]J. F. Scott, Rev. Mod. Phys. 46, 83 (1974).

[27]D. L. Rousseau and S. P. S. Porto, Phys. Rev. Lett. 20, 1354 (1968).

[28]J. F. Scott, Phys. Rev. Lett. 24, 1107 (1970).

[29]P. J. Colwell and M. V. Klein, in *Light Scattering in Solids*, edited by M. Balkanski (Flammarion, Paris, 1971), p. 102.

[30]M. V. Klein, in *Raman Scattering in Solids*, edited by M. Cardona (Springer, New York, 1975).

[31]J. Doehler, P. J. Colwell, and S. A. Solin, Phys. Rev. Lett. 34, 584 (1975).

[32]J. Doehler, Phys. Rev. B 12, 2917 (1975).

[33]D. E. Nixon and G. S. Parry, J. Phys. D 1, 219 (1968).

[34]G. S. Parry and D. E. Nixon, Nature 216, 909 (1967).

[35]G. S. Parry, D. E. Nixon, K. M. Lester, and B. C. Levene, J. Phys. C 2, 2156 (1969).

[36]G. S. Parry, in *Third Conference on Industrial Carbon and Graphite* (Society of Chemistry, London, 1971), p. 58.

[37]See Ref. 1, and references therein.

[38]G. S. Painter and D. E. Ellis, Phys. Rev. B 1, 4747 (1970); also P. R. Wallace, Phys. Rev. 71, 622 (1947).

[39]J. C. Slonczewski and P. R. Weiss, Phys. Rev. 109, 272 (1958).

[40]B. Bach, C. R. Acad. Sci. B 273, 666 (1971).

[41]R. J. Nemanich and S. A. Solin, Bull. Am. Phys. Soc. 21, 339 (1976).